Production of low energy pions by 590 MeV protons in nuclei

by **J. F. Crawford, M. Daum, G. H. Eaton, R. Frosch, J. Garzon**[1]),
H. Hirschmann[2]), **P.-R. Kettle, J. W. McCulloch**[3]) **and E. Steiner**

SIN, Schweizerisches Institut für Nuklearforschung, CH-5234 Villigen, Switzerland

(13. X. 1980)

Abstract. We have measured differential cross sections $d^2\sigma/(d\Omega dT_\pi)$ for the production of charged pions by 590 MeV protons in beryllium, carbon and nickel at pion production angles of 22.5° and 90°, for pion energies from 6 MeV to 35 MeV. At the lowest pion energies the cross sections tend towards zero. From nickel there are more slow π^- than π^+; this is attributed to Coulomb effects.

1. Introduction

Measurements of cross sections for the production of low energy pions are needed for the optimal design of new facilities such as surface muon beams [1] and pionic X-ray detection systems [2], at SIN and similar laboratories. In surface muon beams, the μ^+ from π^+ decays at rest in the pion production target are collected. The relevant pions have typical ranges of a few millimetres in the production target, i.e., kinetic energies of a few MeV. In the new pionic X-ray facilities the experimental target is placed close to the pion production target; again the relevant π^- mesons are those with kinetic energies of a few MeV.

In a recent survey [3] of the literature on pion production by protons in the energy range of the "meson factories" ($400\,\text{MeV} \lesssim T_p \lesssim 800\,\text{MeV}$) only a few published data for pion energies below 20 MeV were found. Measurements at low pion energies are difficult because of the large effects of ionization energy loss, multiple scattering and decay of the produced pions.

We have measured differential cross sections $d^2\sigma/(d\Omega dT_\pi)$ for the production of charged pions by 590 MeV protons in beryllium, carbon and nickel at pion production angles of 22.5° and 90°, for pion energies from 6 MeV to 35 MeV (all quantities in the lab system). We used specially thin pion production targets in the main extracted proton beam of the SIN accelerator. As pion spectrometers we used the secondary beam transport systems $\pi M3$ and $\pi E3$ [4]. These systems are

---

[1]) Present address: Dto Fisica Fundamental, Universidad Autonoma, Madrid-Cantoblanco, Spain.

[2]) Present address: EIR, Eidgenössisches Institut für Reaktorforschung, CH-5303 Würenlingen, Switzerland.

[3]) Present address: Marconi Space and Defence Systems, The Grove, Warren Lane, Stanmore, Middlesex HA7 4LY, England.

suitable for our measurements because they are doubly focusing (i.e. focusing both horizontally and vertically) and thus allow a high signal-to-background ratio in the detector. Also, the channels are equipped with the vacuum system and shielding necessary for our purpose.

2. Experimental method

The layout of the $\pi M3$ (22.5°) channel is shown in Fig. 1. The 590 MeV proton beam was operated at currents ranging from 6 to 102 microampères. Radiation cooled rotating wheel pion production targets [4] with thin foils were used. For the $\pi M3$ measurements the foil thickness was 3 mm for beryllium and 0.2 mm for nickel. The angle θ_1 between the proton beam and the normal to the target foil surface was 67.5° and the angle θ_2 between the central pion trajectory and the normal to the target foil surface was 45°. For the $\pi E3$ (90°) measurements on carbon and nickel the angles θ_1 and θ_2 as defined above were 60° and 30°, respectively. Here a 0.2 mm nickel foil and a 1 mm graphite foil were used. The 90°-beryllium-data were obtained with the standard SIN production target (thickness 6 mm; $\theta_1 = 90°$, $\theta_2 = 0°$).

In the $\pi M3$ channel the vacuum systems of the production target and the pion channel are separated by two 0.4 mm thick aluminium windows at a distance of 9.5 cm from the production target. The $\pi E3$ vacuum chamber is connected without windows to the production target vacuum; in this channel there were
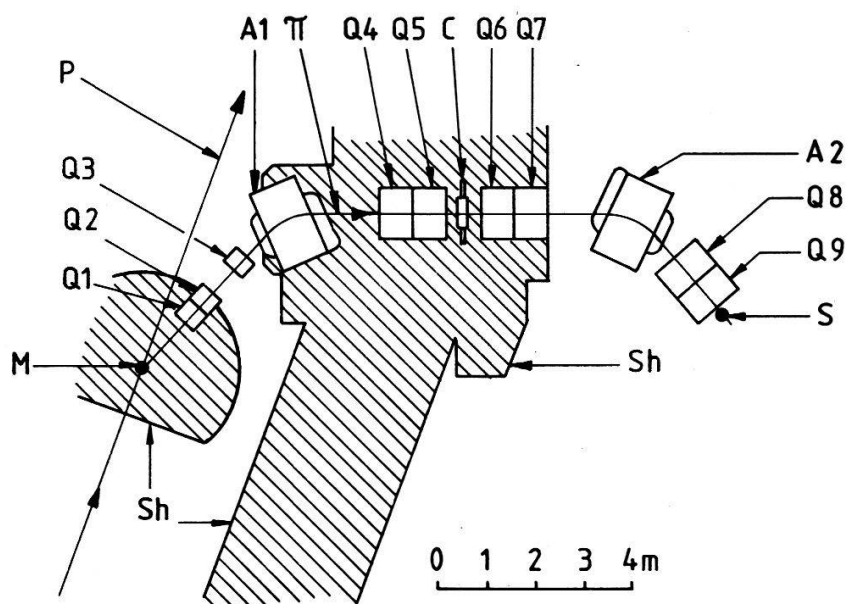

Figure 1
Layout of the $\pi M3$ pion channel used for the measurements at a pion production angle of 22.5°. *M*: pion production target; *p*: 590 MeV proton beam; π: central pion trajectory; Q_i: quadrupole magnets; A_i: dipole magnets; *C*: momentum-defining collimator; *S*: channel end (scintillation counter); *Sh*: shielding (iron and concrete).

0.2 mm mylar windows upstream and downstream of the momentum defining collimator system.

The magnetic pion channels were operated at central momenta from 40 to 102 MeV/c. In $\pi M3$ (see Fig. 1) the momentum was chosen using the bending magnet A_1. The two quadrupole doublets (Q_4, Q_5) and (Q_6, Q_7) were set for an achromatic beam transport from the production target (point M) to the channel end (point S). The triplet (Q_1, Q_2, Q_3) imaged the target point M onto the center C of the momentum-defining colimator. Finally the bending magnet A_2 and the doublet (Q_8, Q_9) were tuned to image point C onto the channel end point S. The channel $\pi E3$ is a similar achromatic system.

At the channel end the pions passed through a 0.1 mm thick mylar vacuum window and were detected in a plastic scintillator. The pions were identified in the large background of electrons or positrons and muons by their pulse height in the scintillator and by their time of flight (TOF) from the production target to the scintillator. The time-to-amplitude converter was started by a pulse in the scintillator and was stopped by the RF signal from the accelerator. Because the SIN proton beam consists of narrow pulses separated by 20 nanoseconds, the TOF method allows one to determine the difference between the particle flight time and an integer multiple of 20 nsec; this is sufficient for our purpose.

The incident proton beam intensity was monitored with pick-up probes [5]. The acceptance of the pion channels was determined using the Monte-Carlo program TURTLE [6], taking into account the magnet settings and apertures of the channel, the energy loss and multiple scattering of the pions in the windows and in the production target, as well as pion decay.

3. Results

The resulting pion production cross sections are presented in Table I and also in Figs. 2 to 6. The quoted pion energies were obtained by adding the energy corresponding to the channel momentum settings and the average energy loss in the production target and, for the $\pi M3$ data, in the vacuum windows. The quoted uncertainties of the cross sections are estimates of the errors in the background subtraction and acceptance calculation; the number of counted pions is so large, that the statistical uncertainties are negligible in all cases. In Figs. 2 to 6 data points from Ref. 3 have been included for comparison. Our data for pion energies above 24 MeV are seen to agree with Ref. 3.

Our data have also been compared with those obtained by Batusov et al. [7]. These authors have used nuclear emulsions to measure $\pi^\pm$ production cross sections of C, Al, Cu and Pb for $T_p = 660$ MeV, $\theta_\pi = 105°$ and T_π down to 11 MeV. For pions of either sign with $T_\pi = 11$ MeV produced in carbon the cross section values of Ref. 7 ($T_p = 660$ MeV, $\theta_\pi = 105°$) are larger than the values interpolated from our data shown in Fig. 3 ($T_p = 600$ MeV, $\theta_\pi = 90°$) by a factor of about 1.6. The discrepancy could at least in part be due to a rise of the cross section with both T_p and θ_π. At higher pion energies the difference between our carbon data at 90° and those of Ref. 7 is smaller (about 10% at $T_\pi = 35$ MeV).

Table 1
Measured nuclear differential cross sections for charged pion production by 590 MeV protons. θ_π:
Pion production angle. T_π: Pion kinetic energy. All quantities in the lab. system.

θ_π		T_π	$d^2\sigma/(d\Omega dT_\pi)$	$\mu b/(\text{sr. MeV})$
degrees	Target	MeV	π^+	π^-
22.5	Be	13.3	2.11±0.46	0.77±0.17
		15.8	2.05±0.35	0.80±0.14
		25.3	4.30±0.73	1.46±0.25
		31.0	5.80±0.99	1.78±0.30
	Ni	11.3	6.0±1.8	6.8±2.0
		14.1	6.9±1.8	7.5±1.9
		24.1	17.6±4.6	12.5±3.3
		30.1	21.4±5.6	11.7±3.0
90	Be	10.9	3.21±0.81	1.04±0.27
		11.4	2.78±0.79	1.28±0.30
		11.8	3.86±0.98	1.31±0.35
		19.4	4.9±1.2	1.56±0.40
		24.6	6.0±1.5	2.12±0.51
		35.0	10.2±2.4	2.80±0.67
	C	7.0	2.48±0.47	1.09±0.13
		7.6	2.85±0.59	1.16±0.14
		8.2	4.06±0.50	1.35±0.17
		17.2	6.81±0.84	1.90±0.23
		22.8	9.5±1.2	2.26±0.28
		33.6	14.1±1.7	2.90±0.36
	Ni	6.4	2.02±0.39	5.63±0.69
		7.1	3.21±0.66	6.59±0.81
		7.8	4.65±0.57	7.92±0.97
		16.9	15.4±1.9	9.4±1.2
		22.6	23.0±2.8	11.7±1.4
		33.5	38.2±4.7	12.4±1.5

4. Conclusions

We conclude from our data that in all three nuclei comparatively few pions
are produced with small kinetic energies. For beryllium and carbon the differen-
tial π^+ production cross section $d^2\sigma/(d\Omega dT_\pi)$ is roughly proportional to the pion
energy T_π for small T_π. This behaviour agrees with the isobar model [8] of pion
production, i.e. with the assumption that the incoming proton undergoes the
reaction $p + N \rightarrow \Delta + N'$ (where N and N' are nucleons) and the pion is created in
the decay of the Δ particle. According to this model [8] the cross section
$d^2\sigma/(d\Omega dT_\pi)$ is proportional to $T_\pi^{1/2}$ for $T_\pi \lesssim 5$ MeV, then rises approximately
linearly with T_π in agreement with our data for the light nuclei. For nickel also,
the T_{π^+} dependence of the measured cross section is compatible with a linearly
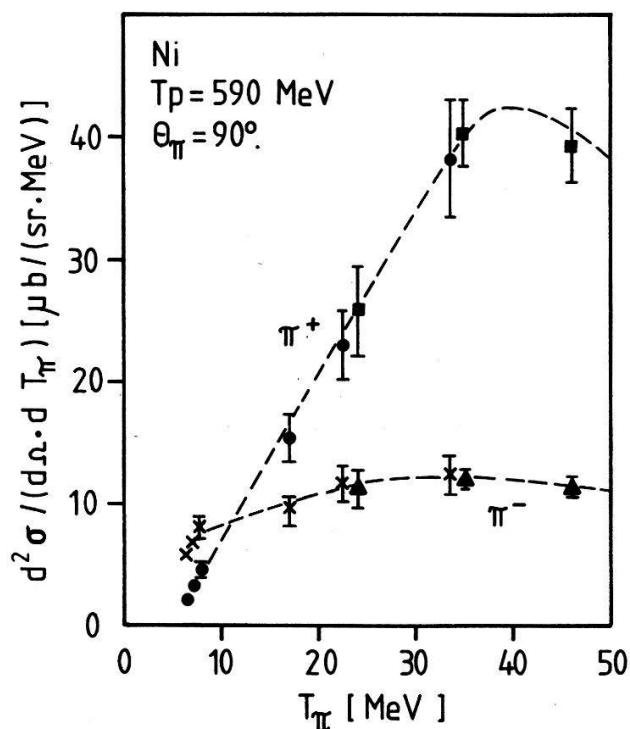rising function of T_{π^+}; however for nickel the best fit straight line crosses the

Figure 2

Measured nuclear differential cross sections for charged pion production by 590 MeV protons in nickel at a pion production angle θ_π of 90°; T_π = pion kinetic energy. There are more π^- than π^+ for $T_\pi \lesssim 10$ MeV. This crossover is attributed to the Coulomb force between the pion and the nuclear protons (see text). The dashed curve has been hand-drawn through the points. The cross sections measured in the present experiment are shown with full circles (π^+) and crosses (π^-); data from Ref. 3 are indicated with squares (π^+) and triangles (π^-).
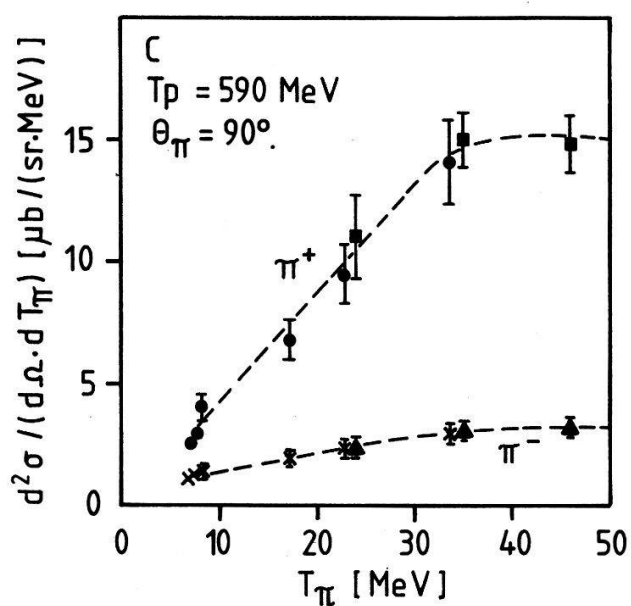

Figure 3

As Fig. 2; cross sections for carbon, $\theta_\pi = 90°$.
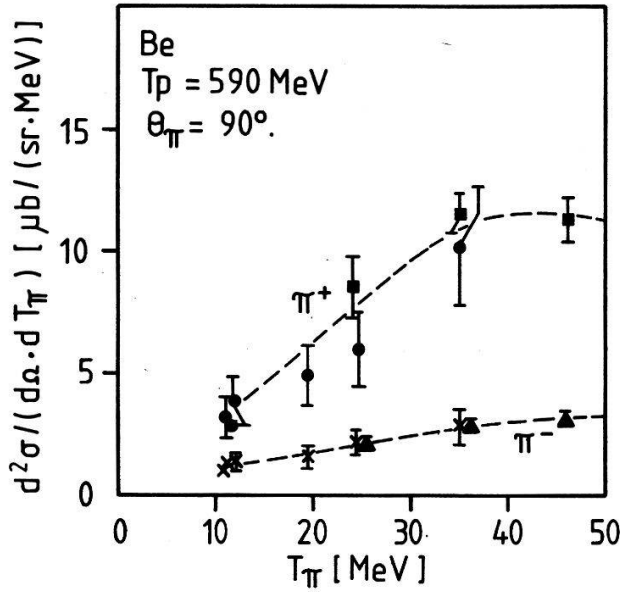
Figure 4
As Fig. 2; cross sections for beryllium, $\theta_\pi = 90°$.

horizontal axis at $T_{\pi^+} \approx +5$ MeV for both production angles (22.5° and 90°), in disagreement with the simple isobar model, from which a slightly negative T_π value for the intercept is predicted. This shift in pion energy can be attributed to the Coulomb repulsion between the π^+ meson and the protons of the residual nucleus; i.e., the T_π dependence of the differential cross section for π^+ production from nickel agrees with the isobar model, as for the lighter nuclei, if the
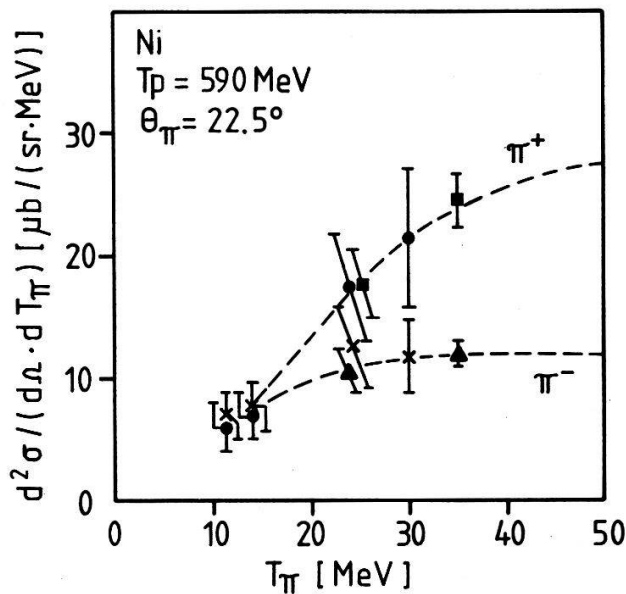

Figure 5
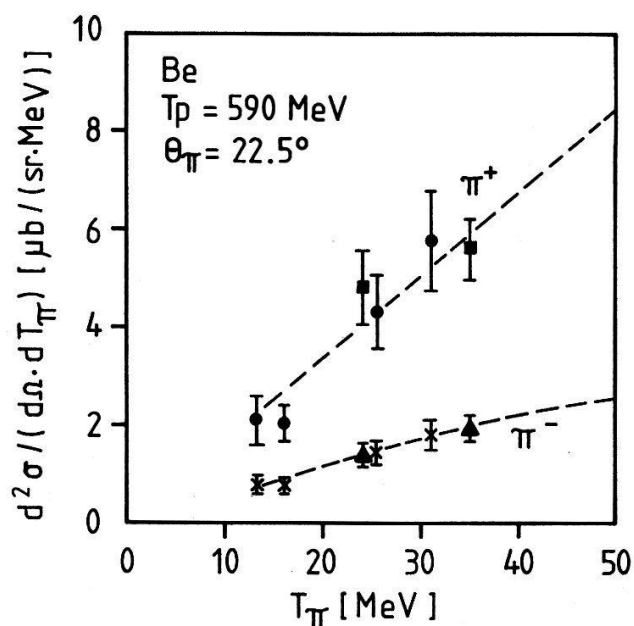As Fig. 2; cross sections for nickel, $\theta_\pi = 22.5°$.

Figure 6
As Fig. 2; cross sections for beryllium, $\theta_\pi = 22.5°$.

estimated pion energy gain from the Coulomb repulsion (about 5 MeV for nickel) is subtracted from the measured pion energy.

The differential cross sections for π^- production are also consistent with a linear rise with the pion energy T_π. The π^- spectra from nickel appear shifted to lower pion energies by a few MeV if compared to the spectra from the lighter nuclei; this can again be attributed to the Coulomb force between the pion and the nuclear protons. As a consequence, at pion energies below about 10 MeV more π^- than π^+ are produced from nickel, whereas for carbon and beryllium the accustomed relative abundance of π^+ and π^- is observed at all pion energies.

The fact that more slow π^- than π^+ are produced from heavy nuclei has been discussed before, e.g. by Kostanashvili et al. [9] who studied the energy spectra of slow π^+ and π^- produced in nuclear emulsion by protons with $T_p = 600$ MeV and 9 GeV and by π^- with T_π (incident) = 60 GeV ($T_{\pi^\pm}$ from 0.5 to 20 MeV; no absolute production cross sections are given). In all cases studied in Ref. 9 the π^- yield is larger than the π^+ yield, e.g. by a factor 10 at $T_\pi \approx 5$ MeV.

The angular distributions of low energy charged pions produced by 590 MeV protons in beryllium and nickel are shown in Fig. 7. These diagrams have been obtained from smooth lines drawn through the data points of this experiment as well as those of Ref. 3. It is seen that slow π^+ predominantly go backward, again in agreement with the isobar model. A weaker backward trend is also observed for π^- produced in beryllium, whereas the π^- from nickel are approximately isotropic. The corresponding π^+ stop densities at the surface of a 5 cm long cylindrical beryllium production target are indicated in Fig. 8. From this figure it is evident that the initial section of a surface muon beam [1] should not be
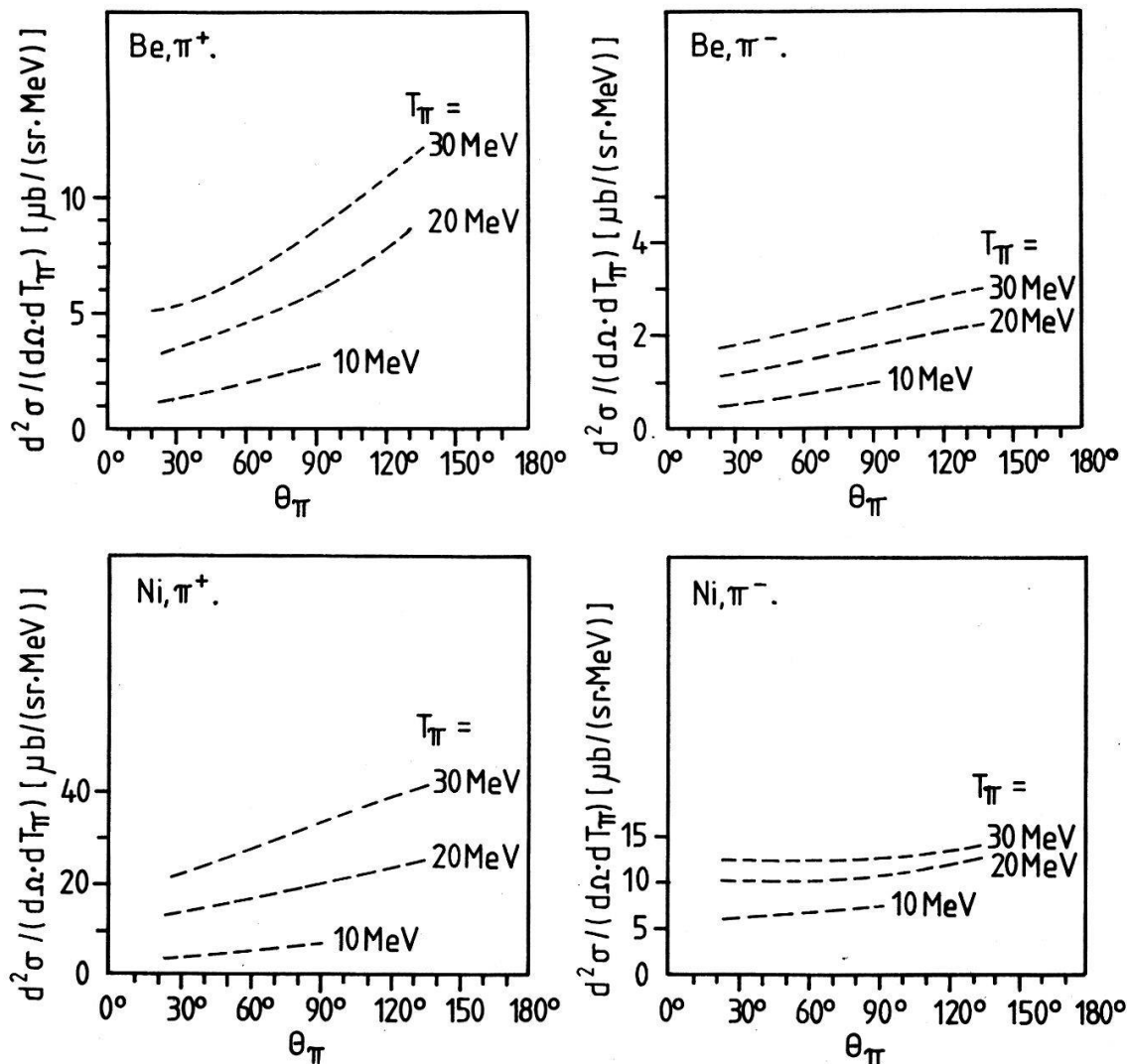
Figure 7

Angular distributions of low energy pions produced in beryllium or nickel by 590 MeV protons. θ_π = pion production angle. T_π = kinetic energy of pion. The curves have been obtained from smooth lines drawn through the data points of Figs. 2 to 6 and through the large angle points of Ref. 3.
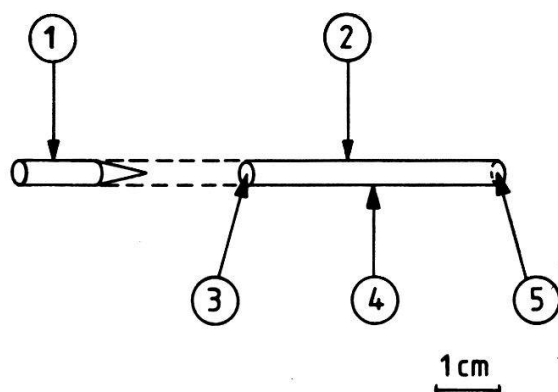

Figure 8

Positive pion stop densities at the surface of a cylindrical beryllium production target. (1) Incident proton beam; $T_p = 590$ MeV. $I = 100 \mu$A; (2) production target; (3) stop density 3.3×10^{10} g^{-1} s^{-1}; (4) stop density 2.5×10^{10} g^{-1} s^{-1}; (5) stop density 1.7×10^{10} g^{-1} s^{-1}. These stop densities have been calculated from the data of this experiment and from Ref. 3, under the assumption of a uniform irradiation with protons on the front face of the target. They imply that comparatively few surface muons go in the forward direction.

oriented in the forward direction. For the design of pionic X-ray facilities according to Ref. 2 it should be kept in mind that due to the Coulomb effect discussed above comparatively many slow π^- are produced from heavy elements.

Acknowledgements

REFERENCES

[1] A. E. PIFER, T. BOWEN and K. R. KENDALL, Nucl. Instr. and Methods *135* (1976) 39.
[2] V. I. MARUSHENKO *et al.*, Pis'ma Zh. Eksp. Teor. Fiz. *23* (1976) 80; translation: JETP letters *23* (1976) 72.
[3] J. F. CRAWFORD *et al.*, Phys. Rev. *C22* (1980) 1184.
[4] SIN users handbook (1972).
[5] R. REIMANN, Journal of Applied Mathematics and Physics ZAMP *25* (1974) 1.
[6] K. L. BROWN and CH. ISELIN, CERN report 74–2 (1974).
[7] YU. A. BATUSOV *et al.*, Yad. Fiz. *26* (1977) 966; translation: Sov. J. Nucl. Phys. *26* (1977) 511.
[8] M. M. STERNHEIM and R. R. SILBAR, Phys. Rev. *D6* (1972) 3117; R. R. SILBAR and M. M. STERNHEIM, Phys. Rev. *C8* (1973) 492.
[9] N. I. KOSTANASHVILI *et al.*, Yad. Fiz. *16* (1972) 983; translation: Sov. J. Nucl. Phys. *16* (1973) 542.